Consideration Of Oil Interaction On The Operating Behaviour Of Twin-Screw Compressors Using Chamber Model Simulations

Matthias HESELMANN*, Lasse BURCHARDT, Andreas BRÜMMER

TU Dortmund University, Chair of Fluidics,
Dortmund, Germany
matthias.heselmann@tu-dortmund.de, andreas.bruemmer@tu-dortmund.de

* Corresponding Author

ABSTRACT

Positive displacement compressors, such as the twin-screw compressor, are frequently oil-injected. The oil brings benefits like partially sealed gap connections, the absorption of a considerable amount of compression heat and the lubrication of the rotors. Even if those basic effects of the oil in the working chambers are well known, predicting them is still a challenge, but needed in terms of optimizing the compressor by simulation. Especially the drawbacks of the injected oil like frictional drag of the oil, or in general hydraulic losses are not fully understood. Based on high-speed imaging of an oil-injected series twin-screw compressor, this work uses various model approaches for the individual loss mechanisms in order to determine the influence of the oil on the compressor performance. The measurement data of the series compressor - recorded in parallel with the high-speed imaging – are used as a reference. A sensitivity analysis of the performance leads to a weighting of the individual oil-induced loss mechanisms.

1. INTRODUCTION

Screw machines are widely used in industrial applications. The reason for this is their high efficiency over a wide load range, low wear and their simple and robust design (Rinder, 1979). They essentially consist of two intermeshing rotors mounted in a housing that closely encloses them. The requirements for the working fluid with regard to purity are decisive for the design of the compressor stage. Especially when there are no restrictions concerning degree of pollution of the working fluid, the most common compressor type is oil-injected. This has several advantages, such as the elimination of a synchronisation gearbox and the seal between the working chambers and bearing areas. The oil also has a favourable effect on the compression process. This means that the operational gaps between moving parts (rotor-rotor, rotor-housing) are partially sealed and a large proportion of the compression heat generated is absorbed.

Historically, it is known that the injection of oil into the working chamber has a positive effect on the efficiency of the compressor. Investigations regarding oil injection were often carried out with the help of experiments. As this is time-consuming and costly, the simulation of injection has been researched for many years. The investigations are focused on mapping the heat transfer of the working medium to the oil (Persson, 1987; Sangfors, 1984), the distribution of the oil in the working chamber of the machine (Harling, 1993; Heselmann et al., 2024) and the hydraulic losses associated with the injection (Deipenwisch, 2000; Vasuthevan & Brümmer, 2019; Nikolov & Brümmer, 2016). What these studies have in common is that they abstract the machine geometry from three-dimensional to zero-dimensional. This means that the working chamber does not have to be modelled completely three-dimensional - which significantly saves computing resources. Instead, mass and energy conservation are used for each phase (e.g. oil, air) and linked to each other via models (e.g. heat transfer or gap flows). This approach is called chamber model simulation.

2. CHAMBER MODEL SIMULATION

The method chosen to calculate the working cycle of a twin-screw machine is called chamber model simulation. First governing equations is the integral conservation of mass:

$$\frac{dM(t)}{dt} = \sum_i \dot{m}_{ri} \tag{1}$$

saying that the mass M within a control volume changes with respect to the time t according to the sum of all i relative mass flow rates $\dot{m}_{ri}$ crossing the surface of the control volume. The integral conservation of energy is given by:

$$\frac{dE(t)}{dt} = \sum_i h_{t,i} \cdot \dot{m}_{ri} - \bar{p}\frac{dV}{dt} + \sum_k \dot{Q}_k - \dot{\Phi} \tag{2}$$

Herein $E(t)$ is the total energy within a control volume V, e.g. the working chamber. $h_t = h + c^2/2$ is the specific total enthalpy containing the flow velocity c and therefore the first sum describes the change in total energy according to enthalpy flow rates through modeled connections. The second term is the power due to the volumetric work with $\bar{p}$ the averaged pressure of the control volume surface. For a diabatic simulation external heat flows $\dot{Q}_k$ are considered by the sum over all heat transfer connections k modeled. Suitable heat transfer models must be implemented for this. $\dot{\Phi}$ considers induced power by shear stresses acting on moving control volume boundaries. The used chamber simulation method is described in more detail in (Grieb & Brümmer, 2022).

2.1 Mass flow models

To calculate the mass flow rates through the connections sub models has to be chosen. As for simulating dry running compressors the mass flow rates are calculated using a flow coefficient α and a theoretical mass flow rate e.g. an isentropic flow through a nozzle:

$$\dot{m} = \alpha \cdot \dot{m}_{th} \tag{3}$$

(Utri, 2021; Grieb & Brümmer, 2022). The variety of models to calculate a two-phase mass flow rate through a connection is huge. An overview of available literature can be found in (Nikolov & Brümmer, 2023). The models deal with separated flows with and without liquid entrainment, compressible and incompressible approaches, two-phase choked and non-homogeneous two-phase flows. However, in this work for connections within the compressor as well as for the discharge opening the two-phase flow is modeled according to (Nikolov & Brümmer, 2023). Herein the flow coefficient takes into account momentum losses due to friction and contraction effects. In accordance with (Chisholm, 1985) and (Morris, 1991), among others, the theoretical mass flow density of the two-phase flow in the narrowest cross-section A results from the laws of conversation of mass and momentum:

$$\left(\frac{\dot{m}}{A}\right)_{th,2ph} = \left(2 \cdot \int_{p_1}^{p_0} v_e \cdot dp\right)^{\frac{1}{2}} \cdot \left({v_{e,t}}^2 - \beta^4 \cdot {v_{e,0}}^2\right) \tag{4}$$

In this calculation an analytical model for the effective specific volume of the two-phase mixture v_e is used. While the index 0 corresponds to the upstream conditions, the index 1 represents the conditions at the narrowest cross-section. In addition to the specific volume of the gaseous and liquid phases, the model to determine the effective specific volume also includes the mass dryness fraction and the velocity slip ratio. β describes the ratio of the cross-sectional areas in cross-section 0 and 1 and is calculated as in (Nikolov & Brümmer, 2023) for non-circular flow cross-sections.

For the other connections (compressor inlet, suction and discharge pipe) a much simpler approach is used. The area of the connection is divided by the volume fraction of the two-phases in the high pressure cavity. The theoretical mass flow density of the gas is then modeled by an isentropic flow as mentioned before:

$$\left(\frac{\dot{m}}{A}\right)_{th,g} = \rho_{lp,s} \cdot \sqrt{2 \cdot (h_{hp} - h_{lp,s})} \tag{5}$$

where index hp represents the high pressure state and lp,s represents the low pressure state assumes to be in the narrowest cross-section calculated with constant entropy. In case the flow is choked, the mass flow density is limited by its critical value. For the liquid phase, the mass flow density is calculated in the same way:

$$\left(\frac{\dot{m}}{A}\right)_{th,l} = \sqrt{2 \cdot \rho_l \cdot (p_{hp} - p_{lp})} \tag{6}$$

To consider the varying amount of liquid within a working chamber the flow is weighted with the volume fraction of the considered phase in the high pressure cavity

$$\dot{m}_g = \alpha \cdot A \cdot \frac{V_{chamber} - V_{liquid}}{V_{chamber}} \cdot \left(\frac{\dot{m}}{A}\right)_{th,g} \tag{7}$$

respectively

$$\dot{m}_l = \alpha \cdot A \cdot \frac{V_{liquid}}{V_{chamber}} \cdot \left(\frac{\dot{m}}{A}\right)_{th,l} \tag{8}$$

where α is the flow coefficient set to the value $\alpha = 0.8$ which is sufficient for many applications (Utri, 2021; Nikolov & Brümmer, 2017). $V_{chamber}$ is the volume of the high pressure working chamber and V_{liquid} the volume occupied in it by a liquid.

2.2 Calculation of hydraulic losses

In this work the hydraulic loss of the oil flooded twin-screw compressor are calculated in a post processing. The models are taken from Deipenwisch (Deipenwisch, 2000). In general the hydraulic losses are divided into three parts. The first one is the power loss due to the acceleration of the injected liquid to circumferential speed at the rotor tip:

$$\dot{\Phi}_{acc} = \frac{1}{2} \cdot \dot{m}_l \cdot (u_t - c_{m,l} \cdot \sin(\varphi))^2 \quad \text{with} \quad c_{m,l} = \frac{\dot{m}_l}{\rho_l \cdot A_{injection}} \tag{9}$$

Herein $\dot{m}_l$ is the injected liquid mass flow rate and u_t the circumferential speed of the rotor tip. At that point there are some variation possible, e.g. it is possible to distribute the liquid mass in any ratio between the main and the gate rotor, to take into account the acceleration of the gas or to inject the liquid in any circumferential direction. This is captured with the angle φ which gives pure radial injection for a value of $\varphi = 0$ and pure circumferential direction with a value of $\varphi = \pi/2$. The mean velocity of the liquid $c_{m,l}$ is calculated according to mass conservation of injected mass flow rate. However, in this work just the liquid mass is accelerated to circumferential speed of the gate rotor tip, due to the injection at the gate rotor. The second power loss occurs due to friction that has to be considered in the clearances because of the significantly higher viscosity compared to gas. Therefore a superposed Couette-Poisseuille flow is applied for the housing and front gaps:

$$\dot{\Phi}_{fric} = \frac{w_c \cdot l_c \cdot \eta \cdot u^2}{h_c} + \frac{\Delta p \cdot h_c \cdot w_c \cdot u}{2} \tag{10}$$

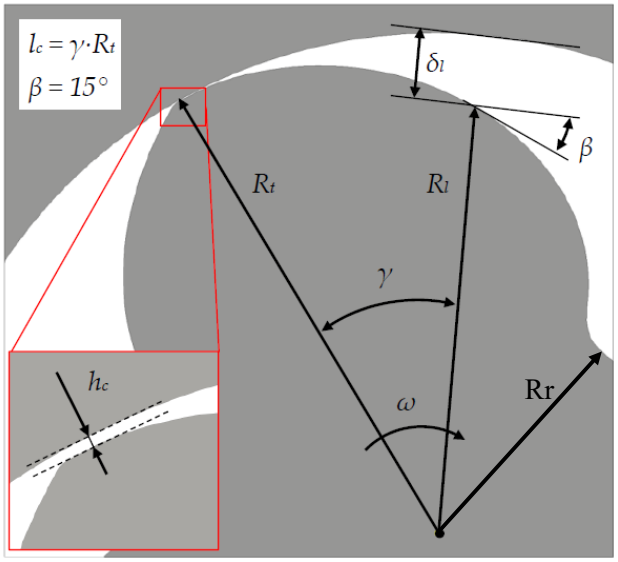

Figure 1: Modelling of the housing clearance in terms of hydraulic loss using the example of the main rotor (Nikolov & Brümmer, 2017).

In the equation, w_c is the width normal to the flow direction, l_c is the effective length in flow direction and h_c is minimum height of the clearance. In figure 1, the determination of the effective length is shown. R_t is the tip radius of the rotor (in this case the main rotor) and R_l is the radius to the rotor surface at which the liquid surge separates from the rotor in front of the gap. The angle β is between the tangent of the rotor tooth and the normal to the radius R_l. The limit value for this angle $\beta = 15°$ results from the assumption of a lubricating film flow, which is only valid for small angles (Harling, 1993). The effective gap length is then determined by the length of the tip radius of the rotor and the angle γ between R_t and R_l. The determination of the effective length is crucial especially for the main rotor housing gap, since the curvature of the rotor favored a slow growth of the angle β and therefore a large effective length. For the other clearances like front gaps and the housing gap of the gate rotor, the angle β hardly enlarges the length of the gaps, since the growth is fast. η is the dynamic viscosity of the injected liquid and u the circumferential speed. For the housing gaps the circumferential speed is the rotor tip speed, for the front gaps however, the circumferential speed is in general a function of the radius $u = u(r)$. For simplicity, in this work the front gaps are considered as one gap reaching from the root circle to the tip circle. Therefore the circumferential speed and length of the clearance is calculated at the mean radius $r = \frac{R_t+R_r}{2}$. The pressure difference over the gap Δp is calculated by the chamber model simulation. The third power loss occurs due to the periodic acceleration of the liquid within the clearance by the passing rotor:

$$\dot{\Phi}_{mom} = \frac{1}{6} \cdot u^3 \cdot \rho_l \cdot h_c \cdot w_c \tag{11}$$

Since the frictional and momentum power loss depends on geometric parameters which change during a working cycle, the power losses are for specific rotor positions. Therefore, the loss has to be integrated over the working cycle which gives the energy for the considered rotor. The energy multiplied with the chamber frequency $f = n \cdot z$, which is the product of the rotational speed n and the number of lobes z of the driven rotor (in this case the main rotor), gives the power loss for the entire compressor.

3. SETUP AND BOUNDARY CONDITIONS

The simulation setup is adapted to an existing test rig of an oil-injected twin-screw compressor. The compressor package BS-62 SLF 75 is provided by BOGE KOMPRESSOREN Otto Boge GmbH & Co. KG. Data of the compressor are given in table 1. However, for simulation purposes the compressor has to be abstracted into a chamber model according to (Grieb & Brümmer, 2022). Therefore, the actual areas of suction and discharge port, as well as the injection area and position are measured and transformed into the chamber model. The complex intermesh clearance is calculated according to (Nadler, 2017). Heat transfer between the gas and oil is not considered in this study. Therefore the simulation of the oil-injected screw compressor using the chamber model simulation is more or less limited to the sealing effect of the oil. The injected oil is modeled as an ideal liquid with constant density and dynamic viscosity. It is stored within a reservoir with constant pressure and temperature. The connection between reservoir and gate rotor chamber is modeled with constant, unity mass flow density, which is adopted to the measured mass flow rate by a coefficient α. The integral of the injected oil through the modeled injection area therefore fits the measured mass flow rate. Constant boundary conditions of the performed chamber model simulations are given in table 2.

Table 1: Compressor data within the test rig (Heselmann et al., 2024)

Designation	Value
nominal power	55 kW
designed pressure ratio	9 - 10
lobe combination	5+6
main rotor wrap angle	300 °
rotor profile	developed by BOGE
diameter ratio (gate/main)	0.8
length to diameter ratio (main)	1.66
inner volume ratio	4.3

Table 2: Boundary condition of the oil-injected compressor (simulation and measurements)

Designation	Symbol	Value
injection position		at gate rotor
injected oil mass	$\dot{m}_{oil}$	≈ 1400 kg/h
oil density	ρ_{oil}	≈ 866 kg/m^3
suction pressure	p_{lp}	0.1 MPa
suction temperature	T_{lp}	≈ 300 K
working fluid		dry Air (ideal gas)
pressure ratio	Π	≈ 7
gap heights	h_c	40 μm - 80 μm

4. RESULTS

Results are splitted into sealing purposes of the oil - included into chamber model simulation and hydraulic losses applied via post-processing. The compressor is modeled adiabatic. Results are presented in terms of delivery rate λ_d:

$$\lambda_d = \frac{\dot{m}}{\dot{m}_{th}} = \frac{\dot{m}}{\rho_{lp} \cdot f \cdot V_{max}} \tag{12}$$

which represents the ratio of the measured or simulated mass flow rate $\dot{m}$ to the theoretical mass flow rate $\dot{m}_{th}$ which can be calculated with the suction density ρ_{lp}, the chamber frequency f and the maximum chamber volume V_{max}. The hydraulic power losses $\dot{\Phi}_{hyd}$ are calculated according to Deipenwisch as described before. The efficiency is evaluated isentropic:

$$\eta_s = \frac{P_s}{P} \tag{13}$$

where P_s is the calculated power of the idealized isentropic compression which delivers the same mass flow rate as the simulated or measured compressor. Therefore P is either the simulated or measured power of the compressor. One

variation parameter is the circumferential Mach number Ma_U:

$$Ma_U = \frac{u}{a_{lp}} \tag{14}$$

which relates the circumferential speed u to the speed of sound at suction conditions a_{lp} of pure air. To investigate the acceleration loss in more detail, the ratio c_m/u between the mean injection velocity c_m and the circumferential speed u is used. When friction is considered the circumferential Reynolds number:

$$Re_U = \frac{\rho_l \cdot u \cdot D}{\eta} \tag{15}$$

is used. It relates the inertia forces to the friction forces, with D as the characteristic length which is the tip diameter of the rotor.

4.1 Variation of oil-distribution

As the aim of this work is to cover oil-injection within a chamber model simulation, the oil distribution is varied first. By using the two-phase mass flow model described by (Nikolov & Brümmer, 2023) the only parameter left to vary is the oil distribution towards the housing of the compressor. When calculating the gap flow through the housing gap this parameter is used to determine the volume fraction of the liquid in the high pressure working chamber, which is located on the housing of the chamber. Depending on the liquid volume in the chamber and the height of the gap, this parameter influences how large the volume fraction of the liquid in the narrowest cross-section of the housing gap is. If the density of the two phases is taken into account, this also influences the mass dryness fraction. Meaning that if this parameter is set to zero no liquid is considered to fill the housing gap of the rotors and therefore the whole amount of oil is homogeneously distributed within the working chambers. Otherwise, part of the injected liquid is used to primary fill the gap volume of the housing gap. The remaining liquid volume is then also distributed homogeneously in the chamber. As shown in figure 2 even a slight distribution of the liquid towards the housing has a huge impact on the delivery rate of the compressor, especially at low circumferential Mach numbers. As the measured data of the delivery rate are included here, it can be concluded, that it is not that important to what extend the liquid is distributed at the housing, but that it is distributed at the housing. Considering higher circumferential Mach numbers it is to mention that the delivery rate of the simulated oil-injected compressor behaves comparable to a dry running compressor. That is because the time for leakage mass flow decrease. Although the amount of injected oil per working chamber decrease too, the delivery rate keep rising with increasing rotational speed. Comparing to the measured data, the delivery rate reaches a maximum at approximately $Ma_U \approx 0.08$. This could be a heat transfer effect which is not considered in this chamber model simulation. This means the oil, which flow back to the suction side of the compressor heats up the sucked in gas, lowering the density of the gas compared to low pressure (ambient) conditions. (Heselmann et al., 2024) show that the oil accumulates in the suction port as well, using high speed imaging. Figure 3 depicts the calculated oil mass within the main and gate rotor working chamber, for an oil distribution towards the housing of 20 % over the rotational angle of the main rotor on the left hand side. Beside the oil mass the connection to the suction port and the injection area is shown. Clearly, the oil mass increases the most when injection takes place, as covered by the simulation. Although injection takes place on the gate rotor side, the amount of oil within the working chambers is nearly equally distributed on both rotors towards the low

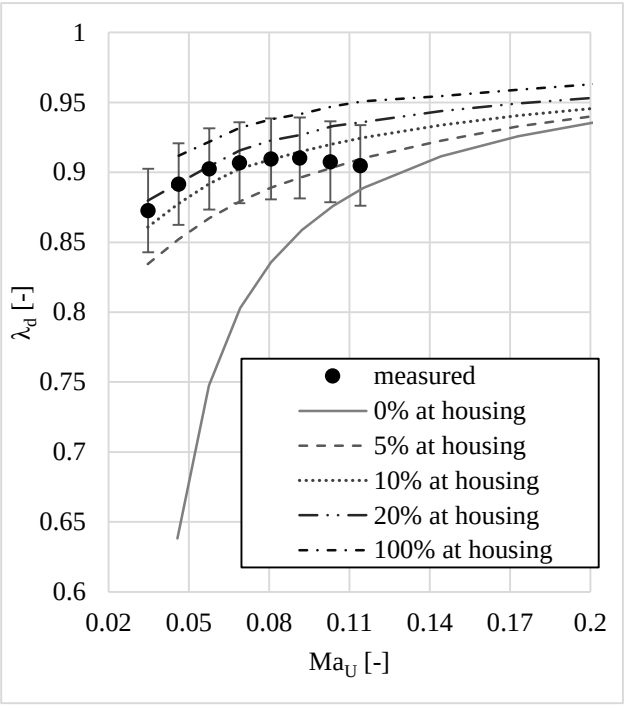

Figure 2: Delivery rate as a function of the circumferential Mach number for a variation of the oil distribution towards the housing.

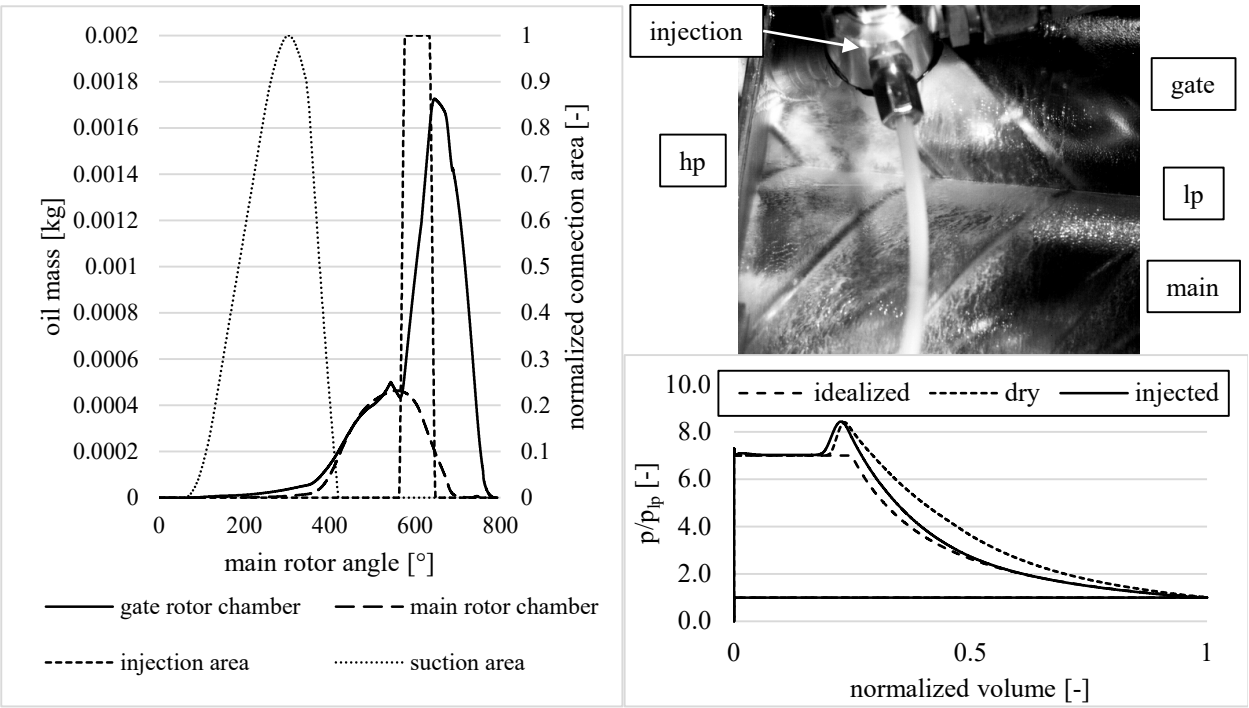

Figure 3: Calculated oil distribution in main and gate rotor chamber over the main rotor angle in comparison to high speed imaging and resulting normalized pV-diagram in comparison to idealized isentropic-isobaric and dry running compressor. 20 % of the oil is distributed towards the housing in the simulations at 50 Hz rotational speed.

pressure side. Even during suction phase the working chambers fill with oil through the gaps. That reflects relatively well the previously shown high speed recordings in (Heselmann et al., 2024). One photo is shown in figure 3 too, taken at a frequency of $n \approx 50$ Hz, a pressure ratio of $\Pi \approx 7$ and an injected oil mass of $\dot{m}_{oil} \approx 1400$ kg/h. This photo focus on the downside of the compressor, where compression and discharge take place. The high pressure side is on the left hand side. The oil is injected at the gate rotor side at a relatively far progressed working cycle. The appearance of the oil is white/foamy when the oil splashes within the chamber or rolls in front of a rotor tooth, because the light is reflected. It seems transparent with a few streaks when the oil surface is relatively smooth like a surface film on the housing. It is documented that the oil distribution within the compressor is by far not equally, but concentrates towards the discharge. However, it seems to be enough oil in the working chamber to form a surge as soon as the suction phase ends, already. Looking now to the normalized pV-diagram also shown in figure 3 it shows the normalized chamber pressure over the normalized volume of the simulated compressor. It includes an idealized compression cycle with isentropic compression and isobaric suction and discharge. The simulations are done for no oil injection (dry) and injection of $\dot{m}_{oil}$ = 1400 kg/h with 20 % of the injected liquid concentrates at the housing, at a frequency of n = 50 Hz. Comparing the compression of the three cycles the sealing effect of the liquid within the working chamber is obvious. Especially at the beginning of the compression the simulation of the injected compressor is almost exactly the isentropic compression which is 100 % sealed. The course of the compression seems plausible, as more and more gap flows can be observed in the experiment as the working cycle progresses (Heselmann et al., 2024).

4.2 Influence on the efficiency

Figure 4 shows the isentropic efficiency for the measured and simulated compressor as a function of the circumferential Mach number. The boundary conditions are given in table 2. For the injected oil the dynamic viscosity is varied. Other mechanical losses, e.g. mechanical losses of the bearings, are not considered here. The injected oil is distributed towards the housing by 20 %. The efficiency shows a quadratic curve with a maximum at $Ma_U \approx 0.06$ in the measured data due to increasing hydraulic losses. The maximum of the simulated inner power P_i is at approximately $Ma_U \approx 0.15$. Since the hydraulic losses are applied in a post processing the reason for this is the discharge throttling. It is increased compared to dry running operation, because the oil reduces the discharge area available for the gas phase. If the hydraulic losses are added, a growing deviation from the measured data can be observed with increasing viscosity. Most

of the deviation from the measured data could be explained by the heat transfer between the oil and the gas. A more or less small deviation would be due to other mechanical losses such as those of the bearings. This underlines the fact that an additional consideration of the heat transfer between the phases is essential for a good simulation of the operating behavior of an oil-injected twin-screw compressor.

4.3 Influence on acceleration power loss

The power loss due to acceleration of the oil depends on the mass flow rate of the injected oil and the need to accelerate the fluid to circumferential speed of the rotor tooth. Therefore, the losses can be modified by changing the direction of the injection towards circumferential direction. Figure 5 depict the acceleration power loss as a function of the circumferential Mach number and the ratio of mean injection velocity to circumferential speed on the left hand side. The injection is in pure radial direction. The quadratic behavior of the power loss with the circumferential Mach number is clearly identified (ref. eqn. 9).

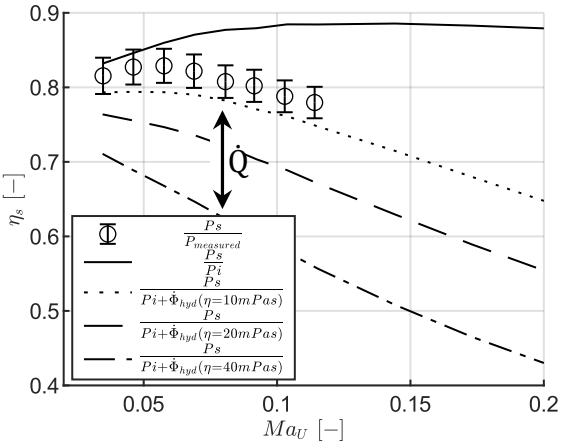

Figure 4: Isentropic efficiency as a function of the circumferential Mach number for measured shaft power, calculated inner power and summation of inner power and hydraulic losses. The dynamic viscosity is varied, the injected oil is concentrated towards the housing by 20 %.

The mean velocity of the oil can by varied by increasing the injected mass flow rate or decrease injection Area. On the right hand side, for a constant circumferential Mach number, the power loss is shown as a function of the velocity ratio and the injection angle. As the power loss vanishes, when the oil is injected with circumferential speed in circumferential direction and reaches negative values in regions where the mean velocity of the oil is faster than the rotor tip, this means that the injected oil accelerates the rotor. The angle to reach the point where no acceleration of the oil is needed ($\dot{\Phi}_{acc} = 0$) decrease with increasing velocity ratio if the oil velocity is faster than the tip speed.

4.4 Influence on frictional power loss

Without changing the geometry, the width, length and height of the clearances, which are dependent on the rotational angle, are also unaffected. Therefore the dynamic viscosity and the circumferential speed remain as influencing parameters since the pressure difference over the connection is a result of the simulation. Expressed in terms of dimensionless numbers the frictional power loss is a function of the circumferential Reynolds number, shown in figure 6a for different dynamic viscosities. The minimum assumed viscosity of 1 mPa·s approximately aligns with the value of water. It can

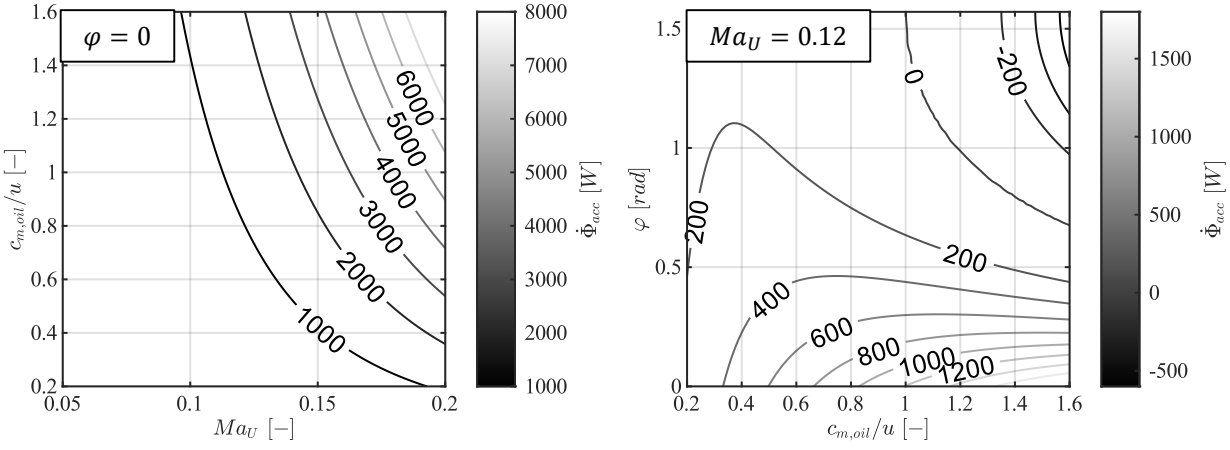

Figure 5: Acceleration power loss as a function of the circumferential Mach number and the ratio of mean velocity of injected oil to circumferential speed (left) and as a function on the velocity ratio and the injection angle φ.

be seen that a higher dynamic viscosity leads to greater power losses caused by shearing of the oil in the gap. When considering the impact of individual gaps, it should be noted that frictional power losses are caused in the housing gap of the main rotor in particular. The large gap area and the high relative speed of the moving boundary, which is the entire circumferential speed of the rotor, contribute to this phenomenon. Due to the larger clearance length the losses in the front gaps of the main rotor are also higher than those of the gate rotor. In addition, smaller clearance heights and greater pressure differences on the high pressure side lead to increased power losses than on the low pressure side.

4.5 Influence on momentum power loss

The momentum power loss due to periodic acceleration of the oil by the passing rotor, can be expressed as a function of the circumferential Mach number and the density of the oil, figure 6b. It has a cubic curse over the circumferential Mach number. The density of the oil has negligible influence on the losses, especially with circumferential Mach numbers of $Ma_U < 0.1$. As with frictional power losses, most of the momentum power loss occur in the housing gap of the main rotor. A comparative analysis of momentum losses within the front gaps reveals that these have a more significant influence on the low-pressure side because of the larger clearance height. However, the assumption of gaps completely filled with oil seems particularly simplifying at this point compared to the high-speed recordings.

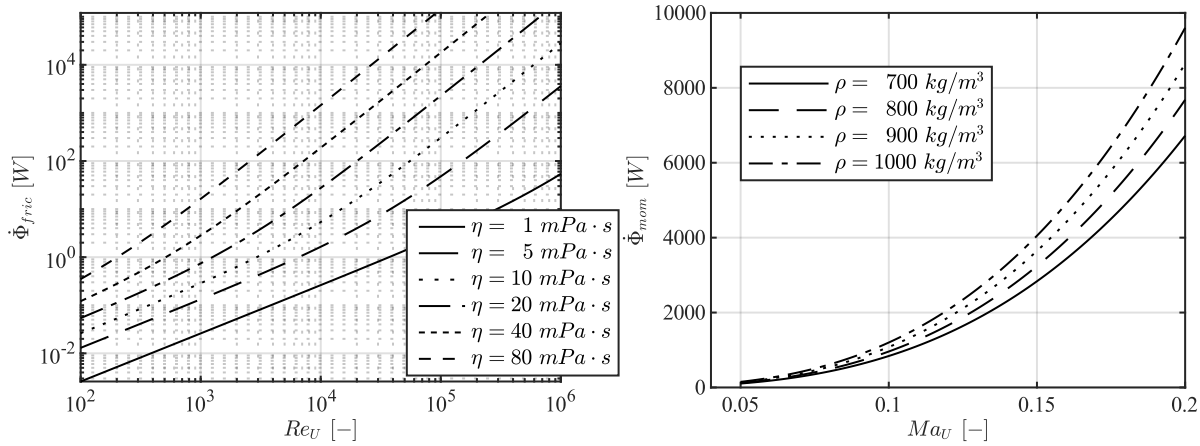

(a) Frictional power loss.

(b) Momentum power loss.

Figure 6: Power loss due to friction as a function of circumferential Reynolds number for different viscosities (a) and power loss due to periodic acceleration as a function of circumferential Mach number for different densities (b).

4.6 Sensitivity

For now the power losses are calculated and the behavior over the circumferential Mach number is shown. Figure 7 depict the portion of the individual loss mechanisms over the circumferential Mach number for different dynamic viscosities. Starting on the left hand side with small dynamic viscosity, comparable to water, the majority of the power loss is the periodic momentum power loss. With increasing circumferential Mach number the portion even rises. That is true in every case, since the circumferential speed has a cubic contribution. However, if the viscosity of the injected fluid increases, the influence of friction losses will quickly outweigh the other loss mechanisms. As the viscosity usually depends strongly on the temperature, there is a great need to model the heat transfer between the phases. It is also important to develop models of fluid distribution to allow for only partial sealing of the gaps. This could for example happen if the frictional power is calculated during the clearance flow simulation. For the sake of completeness, it should be mentioned that the influence of acceleration losses is by far the lowest.

5. CONCLUSION

The simulation of a twin-screw compressor using a chamber model takes into account the conservation of mass and energy and is therefore zero-dimensional. In the present work, the chamber model has been enabled to inject liquids and to transport them through the machine via the existing gap connections. A heat exchange within the working chambers

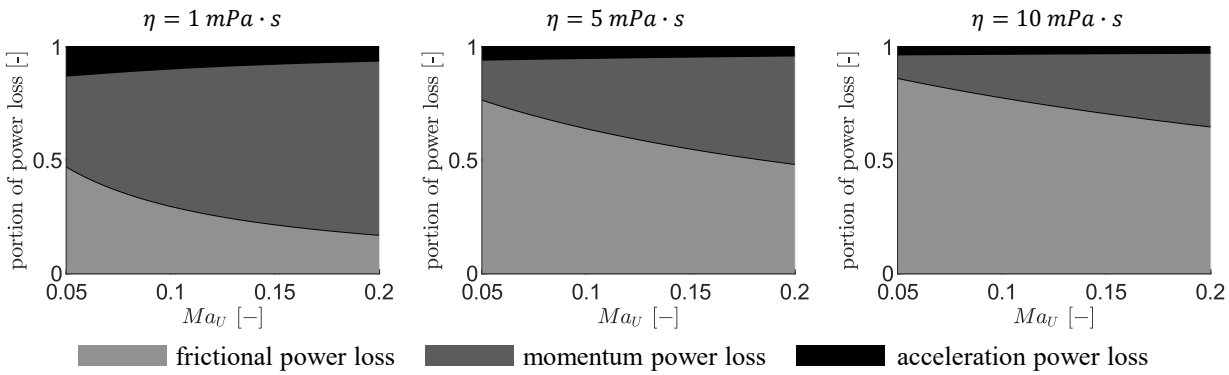

Figure 7: Portion of power loss due to acceleration, friction and momentum as a function of the circumferential Mach number for different dynamic viscosities. The liquid injection of $\dot{m}_{oil}$ = 1400 kg/h is considered in pure radial direction.

between liquid and working medium, which exists in reality, is not considered. It is shown that the injected liquid, in this case oil, is able to seal the gap connections. This is an essential task of the injected liquid. A comparison with measurement data and high-speed images shows that it is important to map a concentration of the oil on the housing wall. A negative effect of the injected oil, causing hydraulic losses, is calculated with a published model in post-processing. This model includes the losses due to oil acceleration after injection as well as the momentum and friction losses in the gaps. All loss mechanisms considered show a strong dependence on the circumferential Mach number, which is partly due to the underlying assumptions, e.g. completely filled gaps. Due to the highest circumferential speed and relatively large effective gap length, the influence of the main rotor housing gap is the one with the greatest influence. If the loss mechanisms are considered, compared to all other loss mechanisms the acceleration losses of around 12 % - 3 % (increasing circumferential Mach number) are the most negligible. The dynamic viscosity of the injected fluid is decisive for the weighting of the friction and momentum losses. From a dynamic viscosity of η = 10 $mPa \cdot s$, the portion of frictional losses is 86 % - 65 % (increasing circumferential Mach number). In order to calculate the power consumption as accurately as the mass flow rate, for future simulation it is therefore necessary to model the oil distribution (which gaps are really completely closed) and the heat transfer between the phases.

NOMENCLATURE

c	velocity	(m/s)	R	radius	(m)
D	diameter	(m)	Re_U	Reynolds number	(-)
E(t)	energy at time	(J)	t	time	(s)
f	chamber frequency	(1/s)	T	temperature	(K)
h	specific enthalpy	(J/kg)	u	circumferential speed	(m/s)
h_c	clearance height	(m)	V	volume	(m^3)
l_c	clearance length	(m)	z	number of lobes	(-)
M(t)	mass at time	(kg)	w_c	clearance width	(m)
$\dot{m}$	mass flow rate	(kg/s)	α	flow coefficient	(-)
Ma_U	Mach number	(-)	β	injection angle	(rad)
n	rotational speed	(1/s)	η	dynamic viscosity	(Pa· s)
$\bar{p}$	average pressure	(Pa)	λ_d	delivery rate	(-)
p	pressure	(Pa)	Π	pressure ratio	(-)
P	power	(W)	ρ	density	(kg/m^3)
Δp	pressure difference	(Pa)	$\dot{\Phi}$	power loss	(W)
$\dot{Q}$	heat flow	(W)	φ	injection angle	(rad)

Subscript

acc	acceleration	m	main
fric	frictional	max	maximum
g	gas phase	mom	momentum
hp	high pressure	r	relative
hyd	hydraulic	r	root
i,k	counting index	s	isentropic
l	liquid phase	t	total
l	lobe	t	rotor tip
lp	low pressure	th	theoretic
m	mean	0,1	state

REFERENCES

Chisholm, D. (1985). Two-phase flow in heat exchangers and pipelines. *Heat transfer engineering*, *6*(2), 48–57.

Deipenwisch, R. (2000). *Ein Beitrag zum Einsatz von Öl als Konstruktionselement in Schraubenmaschinen*. Dissertation University Dortmund.

Grieb, M., & Brümmer, A. (2022). Thermodynamic simulation and experimental validation of an oil-free twin-screw expander. *IOP Conference Series: Materials Science and Engineering*, *1267*(1), 012015. doi: 10.1088/1757-899x/1267/1/012015

Harling, H. B. (1993). *Untersuchung zur Ölverteilung in Schraubenkompressoren mit Schmiermitteleinspritzung*. Dissertation University Dortmund.

Heselmann, M., Dämgen, U., & Brümmer, A. (2024). Experimental Investigation of the Distribution of Two-Phase Flow in Oil-Injected Twin-Screw Compressors. In M. Read, S. Rane, I. Ivkovic-Kihic, & A. Kovacevic (Eds.), *13th international conference on compressors and their systems* (pp. 61–76). Springer Nature Switzerland.

Morris, S. D. (1991). Compressible gas-liquid flow through pipeline restrictions. *Chemical Engineering and Processing: Process Intensification*, *30*(1), 39–44.

Nadler, K. (2017). *Modellierung und Analyse von Schraubenvakuumpumpen im Blower-Betrieb*. Logos Verlag Berlin.

Nikolov, A., & Brümmer, A. (2016). Analysis of Indicator Diagrams of a Water Injected Twin-shaft Screw-type Expander. In *International compressor engineering conference.*

Nikolov, A., & Brümmer, A. (2017). Investigating a Small Oil-Flooded Twin-Screw Expander for Waste-Heat Utilisation in Organic Rankine Cycle Systems. *Energies*, *10*(7), 869. doi: 10.3390/en10070869

Nikolov, A., & Brümmer, A. (2023). Two-phase mass flow rate through restrictions in liquid-flooded twin-screw compressors or expanders. *International Journal of Refrigeration*, *148*, 152–167. doi: 10.1016/j.ijrefrig.2023.01.017

Persson, J.-G. (1987). Heat-exchange in liquid-injected screw-compressors. *Schraubenmaschinen '87. Schraubenverdichter, Schraubenmotoren*.

Rinder, L. (1979). *Schraubenverdichter*. Wien New York: Springer-Verlag.

Sangfors, B. (1984). Computer Simulation of the Oil Injected Twin Screw Compressor. *Purdue University Libraries (Hg.) 1984 – International Compressor Engineering Conference*.

Utri, M. (2021). *Potenzial von nicht-konstanter Rotorsteigung für Schraubenkompressoren*. Berlin: Logos Verlag Berlin.

Vasuthevan, H., & Brümmer, A. (2019). Generic experimental investigation of hydraulic losses within twin-screw machines. *The 9th International Conference on Compressor and Refrigeration*.

ACKNOWLEDGMENT

The authors gratefully acknowledge the German Research Foundation (DFG) for financially supporting this work within the priority program 2403 "Carnot Batteries: Inverse Design from Markets to Molecules" and the research group FOR 5595 "Oil-refrigerant multiphase flows in gaps with moving boundaries - Novel microscopic and macroscopic approaches for experiment, modeling, and simulation".